Solvent-induced Competing Processes in Polycarbonate Degradation: Depolymerization, Chain Scission, and Branching/Crosslinking

Journal:	*Polymer Chemistry*
Manuscript ID	PY-ART-12-2022-001572.R1
Article Type:	Paper
Date Submitted by the Author:	28-Feb-2023
Complete List of Authors:	Sun, Mengqi; Virginia Tech Xu, Zhen; Virginia Polytechnic Institute and State University, Chemistry Munyaneza, Nuwayo Eric; Virginia Tech Zhang, Yue; Virginia Tech Posada, Carlos ; Virginia Tech Liu, Guoliang; Virginia Polytechnic Institute and State University, Department of Chemistry

ARTICLE

Solvent-induced Competing Processes in Polycarbonate Degradation: Depolymerization, Chain Scission, and Branching/Crosslinking

Received 00th January 20xx,
Accepted 00th January 20xx

DOI: 10.1039/x0xx00000x

Mengqi Sun,[a] Zhen Xu,[a] Nuwayo Eric Munyaneza,[a] Yue Zhang,[a] Carlos Posada,[a] Guoliang Liu*[a,b,c]

Poly (bisphenol A carbonate) (PC) is a massively produced engineering plastic and requires innovative recycling methods at its end of life. In this work, we investigate the chemical degradation of PC in dimethylformamide (DMF) and dimethyl sulfoxide (DMSO), catalyzed by copper sulfide nanoparticles (CuS NPs). In DMF, PC is degraded to bisphenol A (BPA) via hydrolytic decomposition with an appreciable yield of ~ 80 %. In contrast, the degradation of PC in DMSO yields oligomeric or branched/crosslinked PC, possibly due to the radical-assisted chain cleavage. Temperature and solution heterogeneity are two parameters that dictate the competition between chain scission and branching/crosslinking. The different degradation behaviors of PC in DMF and DMSO highlight the importance of solvents in polymer degradation, which can lead to different pathways of hydrolytic depolymerization or radical-assisted chain scission, branching, and crosslinking. This work provides new insights into the recycling of plastic wastes and offers new avenues to induce polymer branching/crosslinking.

Introduction

End-of-life plastics pose environmental challenges and spur extensive efforts in recycling.[1-5] Poly(bisphenol A carbonate) (PC), massively produced at 4.5 million tons annually,[6, 7] is one of the most produced engineering plastics. It has wide applications in electronics,[8] construction,[9] automotive,[10, 11] and aircraft[12] owing to its excellent mechanical, thermal, and optical properties.[6, 13-16] The enormous global production exerts urgent needs for effective recycling. Among various recycling approaches,[17-21] chemical recycling holds great promise because it can degrade polymers into easily processable building blocks or valuable chemicals.[22-30] Hydrolysis,[31-40] thermolysis,[41-43] alcoholysis,[44-47] aminolysis,[48, 49] and hydrogenation[50] are among the most extensively investigated approaches.

Hydrolysis of polycarbonate can date back to 1962.[32] The hydrolytic reaction with hydroxide ions converts PC to bisphenol A (BPA) and CO_2.[32, 34, 38] The resulting BPA monomer can be used as a chemical feedstock, enabling the conversation of PC to other engineering plastics.[36] Inorganic catalysts have been used to improve the degradation efficiency because they coordinate with the carbonyl group to enhance its electrophilicity.[31, 35, 37, 39] However, due to the hydrophobic nature of PC, the industrial hydrolysis process requires high-temperature steam to ensure phase compatibility.[6, 34, 40] Judiciously selected solvents can potentially circumvent the energy-intensive approaches and maintain phase compatibility.

Besides hydrolysis, radical-assisted degradation is another effective chemical approach. Radicals are often generated by heat or light. UV photolysis[51, 52] is a common method to generate free radicals for polymer degradation. The high-energy photons cleave the polymer chains and leave radicals in the backbone, which lead to β-chain scission and yield products with smaller molecular weights. The radicals can undergo radical propagation and transfer before recombination to terminate the reaction.[53-60] Since the short-lived radicals can potentially induce polymer branching or crosslinking, there exists a competition between chain scission and chain branching/crosslinking. Only the former leads to polymer degradation to small molecules; the latter can produce high-molecular-weight polymers and possibly be used for polymer modification. For instance, Graebling used thiuram disulfide compounds to suppress β-scission and facilitate branching (grafting) of polypropylene (PP) in the reactive extrusion process.[61] Borsig *et al.* blended PP with polyethylene (PE) as a way to reduce β-scission and achieved crosslinked PP/PE polymer blends.[62] François-Heude *et al.* studied the kinetics of photothermal and thermal oxidation on isotactic polypropylene (iPP) films.[63] They found that with additional hydroperoxide photolysis, chain scission dominated over branching or crosslinking under photothermal conditions.[63] Triacca *et al.* designed both experimental and computational studies on the radical-assisted chain scission of PP and used low concentration of radical initiator to avoid the undesired crosslinking.[64] Ahn *et al.* computationally investigated the radical reactions in PE radio-

---

[a] *Department of Chemistry, Virginia Tech, Blacksburg, Virginia 24061, United states*
[b] *Department of Chemical Engineering, Virginia Tech, Blacksburg, Virginia 24061, United states*
[c] *Department of Materials Science and Engineering, Virginia Tech, Blacksburg, Virginia 24061, United states*
† E-mail: gliu1@vt.edu

Electronic Supplementary Information (ESI) available: Additional EDS, PXRD, GPC, GC-MS, NMR, and DSC results can be found in the Supporting Information. See DOI: 10.1039/x0xx00000x oxidation and found that final products were mainly produced by crosslinking, chain scission, and termination through alcohol and ketone groups.[65] Thus, understanding the competition between polymer chain scission and branching/crosslinking is critical in designing polymer degradation processes.

Herein, we have investigated the degradation of PC in two solvents of dimethylformamide (DMF) and dimethyl sulfoxide (DMSO) (**Fig. 1**). PC underwent hydrolytic depolymerization to produce BPA in DMF and radical-assisted degradation to yield oligomers and branched/crosslinked polymers in DMSO. DMSO can serve as an effective source to generate various radical species.[66-74] To facilitate the radical generation,[75-79] copper sulfide (CuS) nanoparticles (NPs) were synthesized and used as catalysts. The DMSO-generated radicals participated in the chain cleavage reaction, leading to competing processes of oligomerization and branching/crosslinking depending on the reaction temperature and solution heterogeneity.

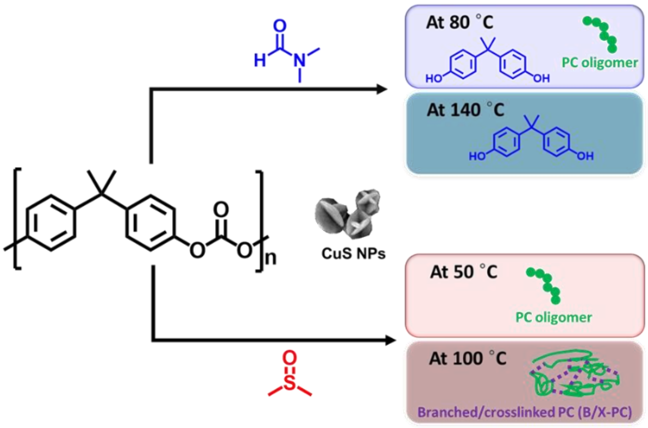

Fig. 1 Scheme of PC degradation in DMF and DMSO.

Experimental

Materials

Bisphenol A-polycarbonate (BPA-PC) was purchased from Lexan (LEXAN^{TM} 123R resin). Dimethyl sulfoxide (DMSO, VWR), anhydrous DMSO (anhydrous 99.9%, Sigma-Aldrich), N-dimethylformamide (DMF, Sigma-Aldrich), anhydrous DMF (anhydrous 99.8%, packaged under Argon, Sigma-Aldrich), hydrogen peroxide (H_2O_2, 30 wt. % in water, ACS reagent grade, Sigma-Aldrich), chloroform (HPLC, Thermo Fisher Scientific), copper nitrate trihydrate ($Cu(NO_3)_2 \bullet 3H_2O$, 98%, Sigma-Aldrich), thiourea (ReagentPlus, >99%, Sigma-Aldrich), ethylene glycol (general lab grade, Thermo Fisher Scientific), polyvinylpyrrolidone (PVP, M_w = 29,000 Da, Sigma-Aldrich), ethanol (VWR), methanol (VWR), and deuterated chloroform ($CDCl_3$, 99.8%, Cambridge Isotope Laboratories, Inc.) were used as received.

Characterization

Number average molecular weight (M_n) of polymers was measured via an EcoSEC HLC-8320GPC Size-exclusion Chromatography (SEC) equipped with two TSKgel SuperHM-H columns, a refractive index detector, and a multiangle light scattering detector (SEC-MALS) at 50 °C. The mobile phase for the SEC-MALS was DMF containing 0.05 M LiBr at a flow rate of 0.5 mL min^{-1}. The specific refractive index increment (dn/dc) of PC in DMF was determined to be 0.14 mL/g. Fourier transform infrared spectroscopy (FTIR) was performed at room temperature using a PerkinElmer ATR-FTIR (model Spectrum 100) in the range of 4000 - 400 cm^{-1} with 128 scans and a resolution of 4.0 cm^{-1}. Gas chromatography-mass spectroscopy (GC-MS) was performed on a 6890 GC with a 5973 Mass Selective Detector (MSD) from Agilent. The MS Wiley library was used to identify the peaks. Separations were performed using the same GC column at the same operating conditions. The MSD transfer line temperature was 260 °C. Chloroform was added as a reference for quantification analysis. Carbon-13 nuclear magnetic resonance (^{13}C NMR) spectroscopy was performed on a Varian Unity 500 spectrometer at 499.98 MHz in $CDCl_3$. Scanning Electron Microscopy (SEM, LEO 1550) at an accelerating voltage of 2 kV and a working distance of ~5 mm was performed to characterize the morphology of the synthesized NPs. Energy-dispersive X-ray Spectroscopy (EDS) was used to analyze the composition of the NPs. Powder X-ray diffraction (PXRD, Rigaku MiniFlex 300/600, Cu Kα = 1.5405 Å) was used to obtain crystallographic information on the synthesized CuS NPs. Differential Scanning Calorimetry (DSC) was performed between 20 °C and 300 °C at a heating/cooling rate of 10 °C/min under a nitrogen stream of 50 mL/min on a Discovery DSC2500 (TA Instruments).

Synthesis of CuS NPs.

First, two precursor solutions of 0.1 M of copper nitrate trihydrate ($Cu(NO_3)_2 \bullet 3H_2O$) and 0.1 M thiourea were prepared in ethylene glycol (EG). In a round-bottom flask (RBF), 0.2 g of PVP was dissolved in 12 mL of EG. Then, 1 mL of 0.1 M $Cu(NO_3)_2 \bullet 3H_2O$ and 2 mL of 0.1 M thiourea EG solution were added to the RBF. The reaction mixture was heated to its boiling point of 197 °C and was kept boiling for 40 min. The solution color changed from colorless to light yellow and then to dark green. The synthesized CuS NPs were collected after five cycles of centrifugation and redispersion in ethanol. In the last cycle, the CuS NPs were dispersed in 10 mL ethanol and then stored in a refrigerator.

Degradation of PC in DMF.

To conduct PC degradation in DMF, PC (50 mg) was first dissolved In DMF (5 mL). From the ethanol solution of CuS NPs, 600 μL was taken and centrifuged in DMF three times. After the last centrifugation, CuS NPs (estimated to be 3.8 mg) were dispersed in the PC in the DMF solution. The mixture was under magnetic stirring of 300 revolutions per minute (rpm) and heated at 80 °C or 140 °C for varying reaction times in the range of 3 to 72 h to initiate the degradation reaction. After the reaction, CuS NPs were separated from the solution via centrifugation before analysis. To analyze the macromolecular PC oligomer products, the oligomers were collected via precipitation by methanol. Reaction in anhydrous DMF was similar, except Schlenk tube was used as the reaction vessel, and nitrogen purging was performed five times to remove moisture.

Homogeneous Degradation of PC in DMSO.

To conduct PC homogeneous degradation in DMSO, PC (50 mg) was added to DMSO (5 mL). After 8 h of magnetic stirring of 300 rpm at 50 °C, PC was only partially dissolved. The undissolved PC was collected via centrifugation, rinsed with methanol, dried in an oven, and weighed to be ~38.9 mg. The dissolved PC was determined to be ~11.1 mg (Table S2). Similar to the degradation of PC in DMF, 600 µL of the CuS/ethanol solution was taken and centrifuged in DMSO three times. After the last centrifugation, CuS NPs were dispersed in the PC in DMSO solution. The mixture was under magnetic stirring of 300 rpm and heated at 50 °C or 100 °C for varying reaction times in the range of 12 to 72 h. After the reaction, CuS NPs were removed via centrifugation. PC oligomers were collected via precipitation by methanol.

Heterogeneous Reaction of PC in DMSO.

Compared to the homogenous degradation of PC in DMSO, a heterogeneous reaction of PC in DMSO was conducted without removing the undissolved PC. PC (50 mg) was added to DMSO (5 mL). In a centrifuge tube, 600 µL of the CuS/ethanol solution was centrifuged in DMSO three times. After the last centrifugation step, CuS NPs were dispersed in the PC in DMSO solution. The solution was under magnetic stirring of 300 rpm and heated at 50 °C or 100 °C for varying reaction times in the range of 6 to 30 h. After the reaction, CuS NPs were removed via centrifugation. Reacted PC polymers were collected via centrifugation and precipitation by methanol.

Results and Discussion

Synthesis and Characterization of CuS NPs.

We have used CuS NPs as the catalysts for PC degradation. CuS was synthesized from precursors of copper nitrate and thiourea in ethylene glycol (EG) at 197 °C using polyvinyl pyridine (PVP) as a surfactant, similar to previous reports.[80-83] The synthesized CuS NPs adopted a hexagonal close-packed (hcp) crystal structure and appeared as anisotropic nanoplates. The nanoplates clustered together and formed three-dimensional "flower-like" structures (**Fig. 2A**). Powder X-ray diffraction (PXRD) (**Fig. 2B**) confirmed the CuS NPs to be hcp covellite, in agreement with the standard, JCPDS No. 06-464. Compositional analysis using energy-dispersive X-ray spectroscopy (EDS) showed an atomic ratio of Cu-to-S close to 1:1 (**Fig. S1**). Particle size analysis showed an average diameter of ~304 nm (**Fig. S2**).

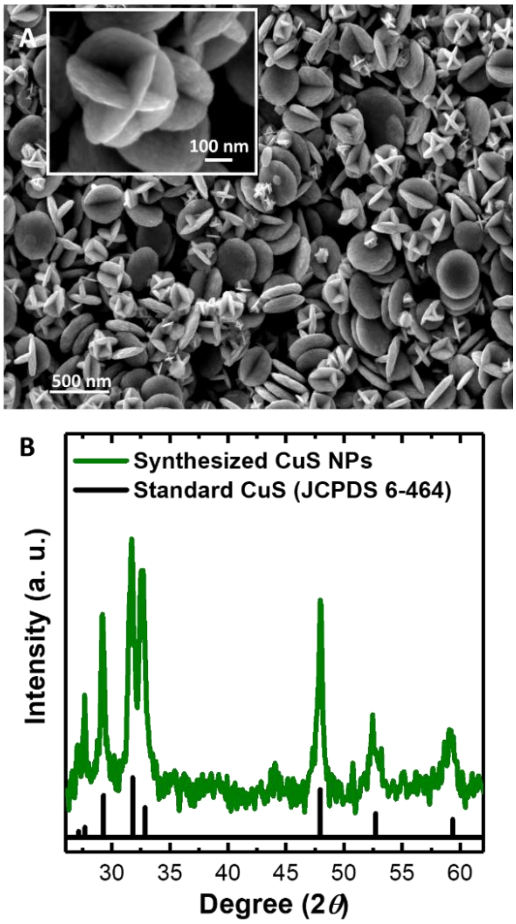

Fig. 2 Characterization of CuS NPs. (A) SEM images of CuS NPs. (B) PXRD pattern of CuS NPs compared with the standard (JCPDS 6-464).

PC Depolymerization in DMF.

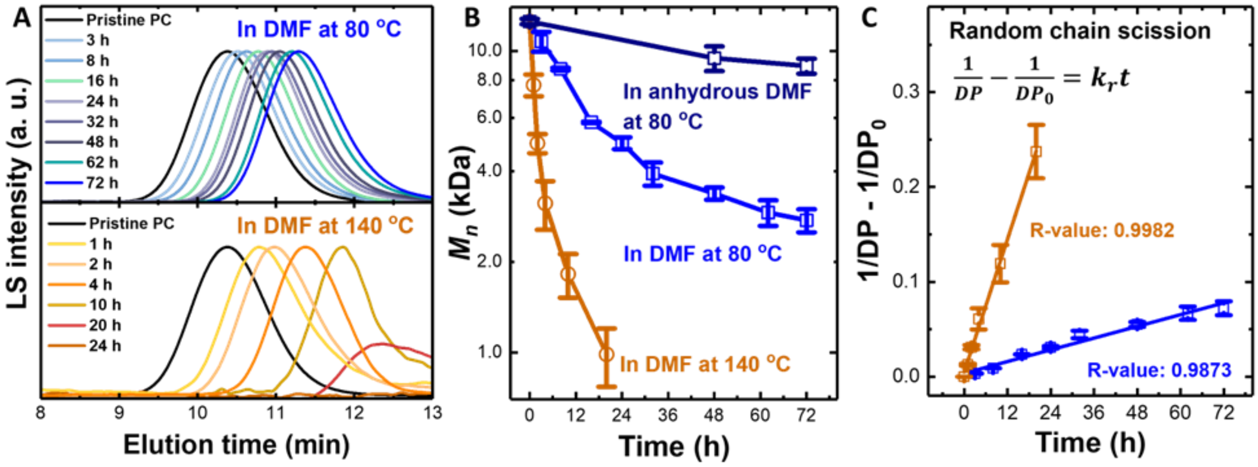

Fig. 3 Reaction kinetics of PC degradation in DMF. (A) GPC traces and (B) M_n evolution of PC degradation in DMF at 80 °C and 140 °C and in anhydrous DMF at 80 °C. (C) PC degradation at 80 °C and 140 °C exhibits a random chain scission mechanism based on the kinetic fitting. Fitting equation and R-values were shown.

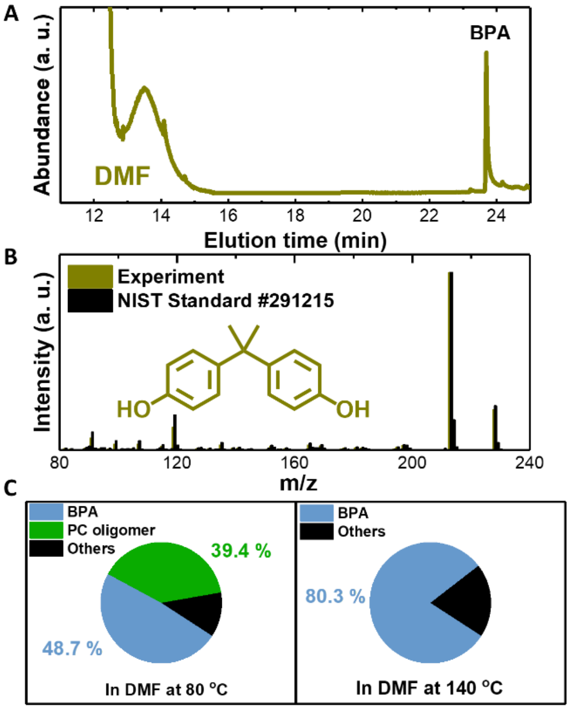

Fig. 4 (A) GC chromatogram, (B) MS spectrum, and (C) BPA yield from the degradation of PC in DMF. PC oligomers were present after degradation in DMF at 80 °C for 72 h but absent at 140 °C for 24 h.

Based on the calculated Flory-Huggins interaction parameters (**Supporting Information**), PC has a higher solubility in DMF than in DMSO, as confirmed by the solubility test (**Table S1** and **Fig. S3**). The different solubilities can lead to different degradation processes of PC in the two solvents. To compare the degradation behaviors in DMF and DMSO, PC degradation was first conducted in DMF at 80 °C and 140 °C. The evolution of PC molecular weight was monitored using gel permeation chromatography (GPC), showing a continuous decline of molecular weight with time (**Fig. 3A**). Only partial degradation was achieved at 80 °C, and a macromolecular component can still be detected by GPC. As evidenced by the decline rate of M_n (**Fig. 3B**), the degradation at 140 °C was much faster, and it reached completion after 24 h without any macromolecular signals detectable by GPC.

To evaluate the importance of catalysts, control experiments of PC degradation without CuS NPs were conducted. PC showed almost no degradation after 72 h at 80 °C and a slight decrease in M_n after 24 h at 140 °C (**Fig. S4**). This observation agrees with previous reports, where inorganic catalysts assisted the hydrolysis of carbonates by coordinating with the carbonyl oxygen to enhance its electropositive character, thus making it susceptible to nucleophilic attack.[33, 37, 39] The proposed catalytic role of CuS NPs was supported by additional control experiments. Carbon nuclear magnetic resonance (^{13}C-NMR) spectroscopy was used to analyze the chemical structures of PC (**Fig. S5**). After PC and CuS NPs were added to DMF or DMSO, we observed a slight downfield shift and therefore deshielding of the carbonyl peak, indicating a slightly lower electron density around carbonyl carbon. This slight deshielding is possibly due to the coordination of carbonyl with CuS NPs.

The degraded compounds in DMF were determined by gas chromatography-mass spectroscopy (GC-MS). BPA was recovered and confirmed by MS (**Fig. 4**). Quantitative analysis showed a BPA yield of ~ 48.7 wt. % at 80 °C and ~ 80.3 wt. % at 140 °C. PC oligomers were collected and determined to be ~ 39.4 wt. % for degradation in DMF after 72 h at 80 °C, in agreement with the GPC characterization. These results suggested that the degradation of PC in DMF involves the cleavage of carbonate and the BPA yield increased with reaction temperature. A small amount of side products was also detected (**Fig. S6**).

The depolymerization of PC in DMF likely follows the hydrolytic decomposition route. Due to the nucleophilicity[84, 85] and tendency to be protonated,[86] DMF can be partially protonated by water to release hydroxide ions, which participate in the nucleophilic reaction with the carbonate group in PC. About 3.7 wt. % of residual water was determined in DMF (**Fig. S7**). During the process, carbon dioxide was released and collected (**Fig. S8**). In the absence of water (*i.e.*, in anhydrous DMF), the M_n decline rate of PC was significantly slower (**Fig. 3B** and **Fig. S9**). About 89.1 wt. % of the PC degradation products in anhydrous DMF were oligomers, with minor side

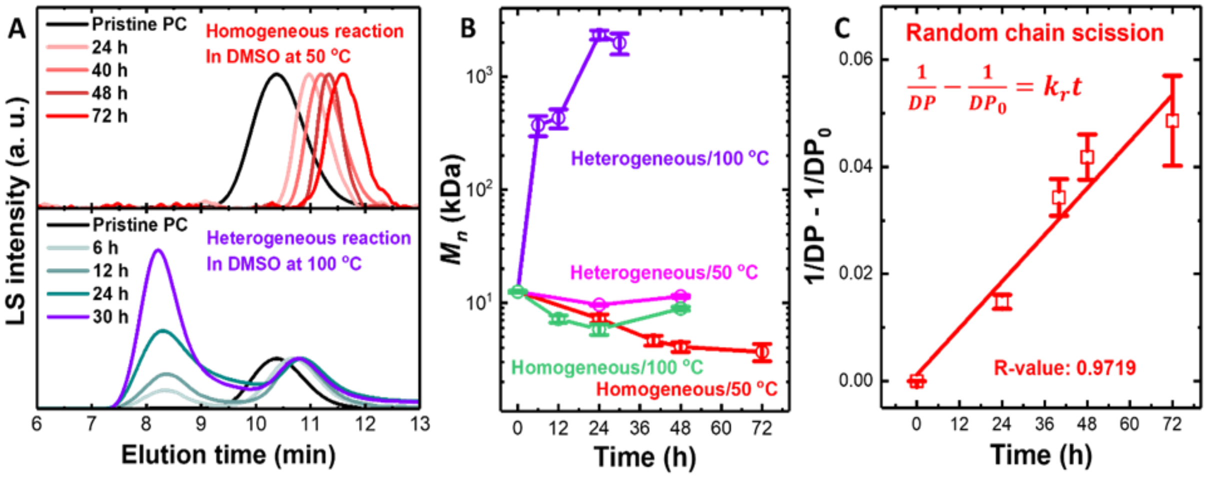

Fig. 5 Reaction kinetics of PC degradation in DMSO. (A) GPC traces of PC homogeneous degradation in DMSO at 50 °C and heterogeneous degradation at 100 °C. (B) M_n Evolution of PC homogeneous and heterogeneous degradation in DMSO at 50 °C and 100 °C. Only homogeneous PC degradation in DMSO at 50 °C showed continuous oligomerization without crosslinking. (C) Kinetic fitting of homogeneous PC degradation in DMSO at 50 °C exhibited a random chain scission mechanism.

products of BPA and carbonates due to the lack of hydroxide ions for carbonate cleavage (**Fig. S10**).

PC Oligomerization and Branching/Crosslinking in DMSO.

In addition to DMF, PC degradation was conducted in DMSO. Because PC has low solubility in DMSO, we first established a homogeneous reaction in DMSO by removing the undissolved PC (**Table S2**). Meanwhile, degradation also proceeds heterogeneously without removing the undissolved PC. The degradation kinetics showed strong dependence on reaction temperature and homogeneity. In a homogeneous solution at 50 °C, PC underwent oligomerization, and M_n decreased continuously as the reaction progressed (**Fig. 5A** and the red curve in **Fig. 5B**). However, at 100 °C and in heterogeneous conditions, GPC traces displayed bimodal patterns. A new GPC peak at a shorter elution time emerged and intensified over time, corresponding to an increased M_n by about 100-fold (**Fig. 5A** and the purple curve in **Fig. 5B**), likely due to chain branching or crosslinking (B/X-PC). To estimate the degree of branching/crosslinking after the heterogeneous reaction of PC in DMSO, B/X-PC was fully dissolved in tetrahydrofuran (THF) and analyzed using GPC. Based on the GPC traces (**Fig. S11**) and comparing the intensities of the two peaks of branched/crosslinked PC and pristine PC, a substantial amount of the polymer chains was branched/crosslinked.

To further probe the effect of reaction temperature and homogeneity, we conducted PC degradation under two more conditions: homogeneous reaction at 100 °C and heterogeneous reaction at 50 °C. The M_n evolutions of both degradation reactions were “V-shaped” (**Fig. 5B**, green and pink curves), suggesting PC chain oligomerization and branching/crosslinking. For the homogeneous reaction at 100 °C, the initial rate of oligomerization was faster than that of the homogeneous reaction at 50 °C (green and red curves). However, the peak position of the GPC trace after the 48-h reaction (**Fig. S12A**) downshifted to a shorter elution time, and another GPC peak appeared at a shorter elution time. The increasing molecular weight implied that polymer branching/crosslinking occurred and escalated over time, which induced the formation of branched/crosslinked PC.

Similarly, for the heterogenous reaction at 50 °C (pink curve), an initial slow oligomerization was followed by the downshifting of the GPC trace and the appearance of a new peak at the lower elution time (**Fig. S12B**). The new GPC peak of the heterogeneous reaction at 50 °C has a smaller intensity and width than that of the homogeneous reaction at 100 °C, implying a lower degree of branching/crosslinking. It is reported that DMSO can generate radicals upon interacting with reactive oxygen species (ROS) or in the presence of a base.[66-74] The radical generation rate depends on temperature following the Arrhenius equation. Upon lowering the reaction temperature from 100 °C to 50 °C, the concentration of radicals decreased, and the number of polymer chain branching/crosslinking events decreased. Hence, the impact of reaction temperature and heterogeneity on the PC degradation behaviors in DMSO can be summarized as follows: high reaction temperature favors both chain scission and branching/crosslinking, and heterogeneity favors the branching/crosslinking only.

To investigate the role of CuS NPs, control experiments without CuS NPs were conducted. PC underwent chain cleavage without CuS NPs, but the reaction rates were drastically slower (**Fig. S13**). Only PC oligomerization was observed in the homogeneous reaction at 50 °C, and branching/crosslinking was present in the heterogeneous reaction at 100 °C. These reactions can be ascribed to the strong tendency of DMSO to generate radicals,[66-74] even in the absence of CuS NP catalysts. However, CuS NPs significantly boosted the radical generation of DMSO through its peroxidase-like behavior to catalyze the generation of ROS,[75-79] which can be intercepted by DMSO to generate other radicals.[66-74] Consequently, PC chain oligomerization and branching/crosslinking were facilitated.

The role of an external initiator was explored by adding hydrogen peroxide (H_2O_2) as a hydroxyl radical (a type of ROS) initiator (**Fig. S14**). With H_2O_2, PC branching/crosslinking was augmented, shifting the competition between chain oligomerization and branching/crosslinking towards the latter. These results consolidated the hypothesis that excessively concentrated radicals could branch/crosslink the polymers rather than degrade them. To pinpoint the chain-scission pathway, we have considered PC degradation in DMF and DMSO following the random chain-scission mechanism or the chain-end scission mechanism.[87] If the degradation follows the random chain scission pathway, the degree of polymerization (DP) should follow the relationship,[87]

$$\frac{1}{DP} - \frac{1}{DP_0} = k_r t \qquad (1)$$

where k_r is the reaction constant, t is the reaction time, and DP_0 is the initial degree of polymerization. If the degradation proceeds according to the chain-end scission mechanism, DP should follow the following relationship,[87]

$$DP_0 - DP = k_e t \qquad (2)$$

where k_e is the reaction constant. Based on the linear fitting of $\frac{1}{DP}$ with respect to time (**Fig. 3C and 5C**), the degradation of PC in both DMF and DMSO adopted the random chain scissions pathway. The

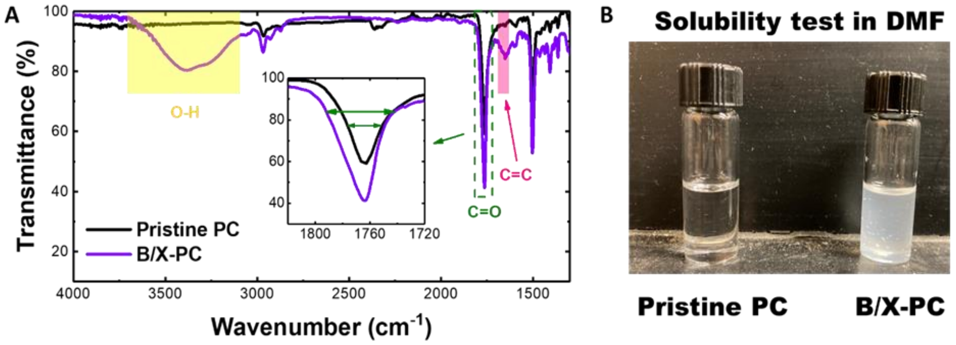

Fig. 6 The branching/crosslinking of PC (B/X-PC) upon heterogeneous reaction in DMSO at 100 °C. (A) FTIR spectra and (B) solubility test in DMF of pristine PC and B/X-PC.

poor fittings of DP with respect to time ruled out the chain-end scission mechanism (**Fig. S15**).

To analyze the backbone structures of PC after oligomerization and branching/crosslinking in DMSO, ^{13}C-NMR was conducted on B/X PC (after heterogeneous reaction at 100 °C), PC oligomers (after homogeneous reaction at 50 °C) and pristine PC (**Fig. S16**). While B/X PC and PC oligomers largely assumed the BPA-based backbone structures of pristine PC, B/X PC showed a new peak at 40.8 ppm. The formation of this new alkyl carbon might be suggestive that the branching/crosslinking occurred at the methyl groups in the backbone of PC.

The chemical structural information of B/X-PC was further evaluated by Fourier-transform infrared spectroscopy (FTIR). After 30 h of heterogeneous degradation reaction at 100 °C, the resulting B/X-PC exhibited several features (**Fig. 6A**): broadening of C=O stretching at 1800-1760 cm^{-1}, the appearance of C=C stretching at 1660-1640 cm^{-1}, and O-H stretching at 3600-3000 cm^{-1}. The formation of alcohol and carbonyl groups could be attributed to the oxidation of carbon-centered radicals. On the one hand, the C=C double bond could result from a disproportionation reaction between two terminating carbon-centered radicals. On the other hand, two terminating carbon-centered radicals may combine, enabling the branching and crosslinking of PC chains.

The PC chain branching/crosslinking endowed the polymers with solvent resistance (**Fig. 6B**). A solubility test of B/X-PC and pristine PC showed that pristine PC was fully soluble in DMF, but B/X-PC could only be partially swollen by DMF. Despite the slightly different solubilities, the thermal property of B/X-PC was much like that of pristine PC, as characterized using differential scanning calorimetry (DSC) (**Fig. S17**).

The different chemical products and branching/cross-linking behaviors confirmed that PC degradation in DMSO was dramatically different from that in DMF. There are three notable differences in the roles of DMSO and DMF in the degradation reactions: (1) PC has a higher solubility in DMF than in DMSO (**Table S1** and **Fig. S3**); (2) DMF acts as a base promoter to partially dissociate water and facilitate the hydrolysis of PC via a nucleophilic reaction;[84-86] (3) DMSO acts as a radical source and supplies reactive radicals to participate in PC degradation,[66-74] but DMF has limited ability to act as a radical source;[66] These differences in the chemical and physical properties of solvents result in different degradation behaviors of PC, that are, hydrolysis in DMF and radical-assisted degradation in DMSO with competing processes of chain scission and branching/crosslinking. The branched and crosslinked PC showed modified chemical and physical properties, such as new functionalities and lower solubility in DMF. Effective degradation of another BPA-based engineering plastic polyetherimide (PEI) in DMSO was also observed as a proof-of-concept of radical-assisted polymer degradation in DMSO (**Fig. S18**).

Conclusions

Here we have reported the degradation of PC in two solvents of DMF and DMSO. Catalyzed by CuS NPs, PC was depolymerized to BPA in DMF via hydrolysis. In DMSO, however, PC underwent radical-assisted chain cleavage to form PC oligomers and/or branched/crosslinked PC (B/X PC). The reaction temperature and heterogeneity played critical roles in the competition between chain oligomerization and branching/crosslinking: Elevated temperatures favor both chain oligomerization and branching/crosslinking because of faster radical generation, while heterogeneous condition favors only chain branching/crosslinking due to strong chain entanglement. The branched/crosslinked PC after degradation in DMSO exhibited reduced solubility in DMF. Insights drawn from the PC degradation in DMF and DMSO can guide future plastic waste recycling, especially in the selection of solvents for degradation. The interesting competition of chain scission and crosslinking/branching induced by radicals can possibly lead to the development of innovative plastic recycling methods. Mechanistic studies of radicals in polymer degradation are currently underway, including detection of radical species, mechanistic pathways, and degradation of other polymers.

Conflicts of interest

There are no conflicts to declare.

Acknowledgements

This work is supported by NSF DMR-1752611 through the CAREER award, NSF Division of Civil, Mechanical, and Manufacturing Innovation (CMMI), and the American Chemical Society Petroleum Research Foundation through the Doctoral New Investigator (DNI) Award. We acknowledged the use of the Nanoscale Characterization and Fabrication Laboratory (NCFL), facilities of the Department of Chemistry at Virginia Tech, Dr. John Matson for access to GPC (THF), and Dr. Mehdi Ashraf-Khorassani for his help on GC-MS instrumentations.

Notes and references

1. A. Chamas, H. Moon, J. J. Zheng, Y. Qiu, T. Tabassum, J. H. Jang, M. Abu-Omar, S. L. Scott and S. Suh, *ACS Sustain. Chem. Eng.*, 2020, **8**, 3494-3511.
2. D. K. A. Barnes, F. Galgani, R. C. Thompson and M. Barlaz, *Philos. Trans. R. Soc.*, 2009, **364**, 1985-1998.
3. P. Dwivedi, P. K. Mishra, M. K. Mondal and N. Srivastava, *Heliyon*, 2019, **5**, No. e02198.
4. J. R. Jambeck, R. Geyer, C. Wilcox, T. R. Siegler, M. Perryman, A. Andrady, R. Narayan and K. L. Law, *Science*, 2015, **347**, 768-771.
5. B. M. Weckhuysen, *Science*, 2020, **370**, 400-401.
6. J. G. Kim, *Polym. Chem.*, 2020, **11**, 4830-4849.
7. Covestro, *Polycarbonates demand worldwide from 2011 to 2021 (in million tons)*, Statista, 2022.
8. *North America Polycarbonate For Electrical and Electronics Market Size, Share & Trends Analysis Report* 2021.
9. K. Schwartz, *Polycarbonates in Construction*, 2015.
10. T. Hotaka, F. Kondo, R. Niimi, F. Togashi and Y. Morita, *Polym. J.*, 2019, **51**, 1249-1263.

11. *Automotive Polycarbonate Glazing Market - Global Industry Analysis, Size, Share, Growth, Trends, and Forecast, 2019 - 2027*, New York, 2019.
12. H. Abramowitz, T. Hentea, Y. Kin and Y. Xu, *Ageing of Materials and Methods for the Assessment of Lifetimes of Engineering Plant - Cape '97*, 1997, 309-317.
13. H. de Brouwer, J. van den Bogerd and J. Hoover, *Eur. Polym. J.*, 2015, **71**, 558-566.
14. M. Scharfenberg, J. Hilf and H. Frey, *Adv. Funct. Mater.*, 2018, **28**, 1704302.
15. E. Bormashenko, R. Pogreb, O. Stanevsky, Y. Bormashenko, Y. Socol and O. Gendelman, *Polym. Adv. Technol.*, 2005, **16**, 299-304.
16. G. Gomez-Gras, M. D. Abad and M. A. Perez, *Polymers*, 2021, **13**, 3669.
17. X. J. Bai, D. H. Isaac and K. Smith, *Polym. Eng. Sci.*, 2007, **47**, 120-130.
18. L. Delva, K. Ragaert, J. Degrieck and L. Cardon, *Polymers*, 2014, **6**, 2912-2927.
19. F. Elmaghor, L. Y. Zhang, R. Fan and H. Q. Li, *Polymer*, 2004, **45**, 6719-6724.
20. W. B. Ding, J. Liang and L. L. Anderson, *Energy & Fuels*, 1997, **11**, 1219-1224.
21. K. Ragaert, L. Delva and K. Van Geem, *J. Waste Manag.*, 2017, **69**, 24-58.
22. M. H. Zeng, Y. H. Lee, G. Strong, A. M. LaPointe, A. L. Kocen, Z. Q. Qu, G. W. Coates, S. L. Scott and M. M. Abu-Omar, *ACS Sustain. Chem. Eng.*, 2021, **9**, 13926-13936.
23. G. Celik, R. M. Kennedy, R. A. Hackler, M. Ferrandon, A. Tennakoon, S. Patnaik, A. M. LaPointe, S. C. Ammal, A. Heyden, F. A. Perras, M. Pruski, S. L. Scott, K. R. Poeppelmeier, A. D. Sadow and M. Delferro, *ACS Cent. Sci.*, 2019, **5**, 1795-1803.
24. F. Zhang, M. H. Zeng, R. D. Yappert, J. K. Sun, Y. H. Lee, A. M. LaPointe, B. Peters, M. M. Abu-Omar and S. L. Scott, *Science*, 2020, **370**, 437-441.
25. B. A. Abel, R. L. Snyder and G. W. Coates, *Science*, 2021, **373**, 783-789.
26. Z. Xu, F. Pan, M. Sun, J. Xu, N. E. Munyaneza, Z. L. Croft, G. Cai and G. Liu, *Proc. Natl. Acad. Sci. U.S.A*, 2022, **119**, e2203346119.
27. A. Rahimi and J. M. Garcia, *Nat. Rev. Chem.*, 2017, **1**, 0046.
28. I. Vollmer, M. J. F. Jenks, M. C. P. Roelands, R. J. White, T. van Harmelen, P. de Wild, G. P. van der Laan, F. Meirer, J. T. F. Keurentjes and B. M. Weckhuysen, *Angew. Chem., Int. Ed. Engl.*, 2020, **59**, 15402-15423.
29. H. Zhou, Y. Ren, Z. H. Li, M. Xu, Y. Wang, R. X. Ge, X. G. Kong, L. R. Zheng and H. H. Duan, *Nat. Commun.*, 2021, **12**, 4679.
30. L. T. J. Korley, T. H. Epps, B. A. Helms and A. J. Ryan, *Science*, 2021, **373**, 66-69.
31. T. Yoshioka, K. Sugawara, T. Mizoguchi and A. Okuwaki, *Chem. Lett.*, 2005, **34**, 282-283.
32. G. D. Cooper and B. Williams, *J. Org. Chem.*, 1962, **27**, 3717-3720.
33. E. Quaranta, *Appl. Catal. B: Environ.*, 2017, **206**, 233-241.
34. H. Tagaya, K. Katoh, J. Kadokawa and K. Chiba, *Polym. Degrad. Stab.*, 1999, **64**, 289-292.
35. G. Grause, R. Karrbrant, T. Kameda and T. Yoshioka, *Ind. Eng. Chem. Res.*, 2014, **53**, 4215-4223.
36. G. O. Jones, A. Yuen, R. J. Wojtecki, J. L. Hedrick and J. M. Garcia, *Proc. Natl. Acad. Sci. U.S.A.*, 2016, **113**, 7722-7726.
37. F. Iannone, M. Casiello, A. Monopoli, P. Cotugno, M. C. Sportelli, R. A. Picca, N. Cioffi, M. M. Dell'Anna and A. Nacci, *J. Mol. Catal. A Chem.*, 2017, **426**, 107-116.
38. A. Ikeda, K. Katoh and H. Tagaya, *J. Mater. Sci.*, 2008, **43**, 2437-2441.
39. G. Grause, K. Sugawara, T. Mizoguchi and T. Yoshioka, *Polym. Degrad. Stab.*, 2009, **94**, 1119-1124.
40. M. Watanabe, Y. Matsuo, T. Matsushita, H. Inomata, T. Miyake and K. Hironaka, *Polym. Degrad. Stab.*, 2009, **94**, 2157-2162.
41. C. Puglisi, L. Sturiale and G. Montaudo, *Macromolecules*, 1999, **32**, 2194-2203.
42. M. Day, J. D. Cooney, C. Touchette-Barrette and S. E. Sheehan, *J. Anal. Appl. Pyrolysis*, 1999, **52**, 199-224.
43. B. N. Jang and C. A. Wilkie, *Polym. Degrad. Stab.*, 2004, **86**, 419-430.
44. L. C. Hu, A. Oku and E. Yamada, *Polymer*, 1998, **39**, 3841-3845.
45. A. Oku, S. Tanaka and S. Hata, *Polymer*, 2000, **41**, 6749-6753.
46. D. Kim, B. K. Kim, Y. M. Cho, M. Han and B. S. Kim, *Ind. Eng. Chem. Res.*, 2009, **48**, 685-691.
47. E. Quaranta, C. C. Minischetti and G. Tartaro, *ACS Omega*, 2018, **3**, 7261-7268.
48. R. Arai, K. Zenda, K. Hatakeyama, K. Yui and T. Funazukuri, *Chem. Eng. Sci.*, 2010, **65**, 36-41.
49. S. Hata, H. Goto, E. Yamada and A. Oku, *Polymer*, 2002, **43**, 2109-2116.
50. S. Westhues, J. Idel and J. Klankermayer, *Sci. Adv.*, 2018, **4**, No. eaat9669.
51. M. Diepens and P. Gijsman, *Polym. Degrad. Stab.*, 2007, **92**, 397-406.
52. J. E. Pickett, *Polym. Degrad. Stab.*, 2011, **96**, 2253-2265.
53. G. Gryn'ova, J. L. Hodgson and M. L. Coote, *Org. Biomol. Chem.*, 2011, **9**, 480-490.
54. L. M. Smith, H. M. Aitken and M. L. Coote, *Acc. Chem. Res.*, 2018, **51**, 2006-2013.
55. J. L. Bolland, *Proc. R. Soc. Lond. A Math. Phys. Sci.*, 1946, **186**, 218-236.
56. J. L. Bolland and G. Gee, *Trans. Faraday Soc.*, 1946, **42**, 236-243.
57. J. L. Bolland and G. Gee, *Trans. Faraday Soc.*, 1946, **42**, 244-252.
58. J. L. Bolland and P. Tenhave, *Trans. Faraday Soc.*, 1947, **43**, 201-210.
59. J. L. Bolland, *Trans. Faraday Soc.*, 1948, **44**, 669-677.
60. J. L. Bolland, *Trans. Faraday Soc.*, 1950, **46**, 358-368.
61. D. Graebling, *Macromolecules*, 2002, **35**, 4602-4610.
62. E. Borsig, A. Fiedlerova, L. Rychla, M. Lazar, M. Ratzsch and G. Haudel, *J. Appl. Polym. Sci.*, 1989, **37**, 467-478.
63. A. Francois-Heude, E. Richaud, E. Desnoux and X. Colin, *J. Photochem. Photobiol. A: Chem.*, 2015, **296**, 48-65.
64. V. J. Triacca, P. E. Gloor, S. Zhu, A. N. Hrymak and A. E. Hamielec, *Polym. Eng. Sci.*, 1993, **33**, 445-454.
65. Y. Ahn, G. Roma and X. Colin, *Macromolecules*, 2022, **55**, 8676-8684.
66. C. L. Opstad, T. B. Melo, H. R. Sliwka and V. Partali, *Tetrahedron*, 2009, **65**, 7616-7619.
67. Y. C. Zhu, Z. Y. Zhang, R. Jin, J. Z. Liu, G. Q. Liu, B. Han and N. Jiao, *Angew. Chem., Int. Ed. Engl.*, 2020, **59**, 19851-19856.

68. R. Herscu-Kluska, A. Masarwa, M. Saphier, H. Cohen and D. Meyerstein, *Chem. Eur. J.*, 2008, **14**, 5880-5889.

69. X. Jiang, C. Wang, Y. W. Wei, D. Xue, Z. T. Liu and J. L. Xiao, *Chem. Eur. J.*, 2014, **20**, 58-63.

70. J. Jia, Q. Jiang, A. Zhao, B. Xu, Q. Liu, W. P. Luo and C. C. Guo, *Synthesis-Stuttgart*, 2016, **48**, 421-428.

71. M. K. Eberhardt and R. Colina, *J. Org. Chem.*, 1988, **53**, 1071-1074.

72. G. A. Russell and S. A. Weiner, *J. Org. Chem.*, 1966, **31**, 248-251.

73. M. J. Burkitt and R. P. Mason, *Proc. Natl. Acad. Sci. U.S.A.*, 1991, **88**, 8440-8444.

74. L. M. Bellotindos, M. H. Lu, T. Methatham and M. C. Lu, *Environ. Sci. Pollut. Res.*, 2014, **21**, 14158-14165.

75. J. F. Guan, J. Peng and X. Y. Jin, *Anal. Methods*, 2015, **7**, 5454-5461.

76. Y. X. Xie, Y. Qian, Z. X. Li, Z. C. Liang, W. F. Liu, D. J. Yang and X. Q. Qiu, *ACS Sustain. Chem. Eng.*, 2021, **9**, 6479-6488.

77. Y. X. Xie, C. C. Gan, Z. X. Li, W. F. Liu, D. J. Yang and X. Q. Qiu, *ACS Biomater. Sci. Eng.*, 2022, **8**, 560-569.

78. Z. J. Yang, Y. Cao, J. Li, M. M. Lu, Z. K. Jiang and X. Y. Hu, *ACS Appl. Mater. Interfaces*, 2016, **8**, 12031-12038.

79. P. L. Li, M. Wang, M. Z. Jiang, W. J. Lai, J. J. Li, K. L. Liu, H. L. Li and C. L. Hong, *New J. Chem.*, 2022, **46**, 13963-13970.

80. M. Q. Sun, N. Kreis, K. X. Chen, X. Q. Fu, S. Guo and H. Wang, *Chemistry of Materials*, 2021, **33**, 8546-8558.

81. M. Q. Sun, X. Q. Fu, K. X. Chen and H. Wang, *ACS Appl. Mater. Interfaces*, 2020, **12**, 46146-46161.

82. H. L. Cao, X. F. Qian, C. Wang, X. D. Ma, J. Yin and Z. K. Zhu, *Journal of the American Chemical Society*, 2005, **127**, 16024-16025.

83. Q. W. Tian, M. H. Tang, Y. G. Sun, R. J. Zou, Z. G. Chen, M. F. Zhu, S. P. Yang, J. L. Wang, J. H. Wang and J. Q. Hu, *Advanced Materials*, 2011, **23**, 3542-3547.

84. G. K. S. Prakash, H. Vaghoo, C. Panja, V. Surampudi, R. Kultyshev, T. Mathew and G. A. Olah, *Proc. Natl. Acad. Sci. U.S.A.*, 2007, **104**, 3026-3030.

85. M. M. Heravi, M. Ghavidel and L. Mohammadkhani, *RSC Adv.*, 2018, **8**, 27832-27862.

86. M. A. Krestyaninov, M. G. Kiselev and L. P. Safonova, *Russ. J. Phys. Chem.*, 2015, **89**, 608-615.

87. R. H. Boyd, in *Thermal Stability of Polymers*, ed. R. T. Conley, Marcel Dekker Inc., New York, 1970, vol. 1.